의학석사학위논문

국소형 자가면역 췌장염과 췌장선암의 감별진단: 역동적 조영증강 자기공명 영상에서 동맥기를 중심으로 병변 대조도의 정량적 비교 연구

Differential diagnosis of focal-type autoimmune
pancreatitis and pancreatic ductal adenocarcinoma:
quantitative comparison of lesion contrast
at dynamic contrast-enhanced MR imaging
with emphasis on arterial phase

울산대학교 대학원

의 학 과

권 지 혜

국소형 자가면역 췌장염과 췌장선암의 감별진단: 역동적 조영증강 자기공명 영상에서 동맥기를 중심으로 병변 대조도의 정량적 비교 연구

지도교수 김 진 희

이 논문을 의학석사학위 논문으로 제출함

2018 년 12 월

울산대학교 대학원

의 학 과

권 지 혜

권지혜의 의학석사학위 논문을 인준함

심사위원　변　재　호　인

심사위원　이　승　수　인

심사위원　김　진　희　인

울 산 대 학 교　　대 학 원

2 0 1 8 년　　1 2 월

Abstract

Purpose: To quantitatively compare the lesion contrast between focal-type autoimmune pancreatitis (AIP) and pancreatic ductal adenocarcinoma (PDA) using dynamic contrast-enhanced MR imaging (DCE-MRI) with emphasis on the arterial phase (AP), and to assess diagnostic performance of the lesion contrast at AP (Contrast$_{AP}$) in differentiating the two diseases.

Materials and methods: Thirty-six patients with focal-type AIP and 72 patients with surgically resected PDA were included, who underwent DCE-MRI including unenhanced, arterial, portal, and delayed phase. The signal intensity (SI) of the mass and normal pancreas was measured at each phase. The lesion contrast (SI$_{pancreas}$/SI$_{mass}$) at each phase was compared between AIP and PDA groups. The area under receiver operating characteristic curve (AUROC) of the lesion contrast at each phase was compared. The sensitivity and specificity of Contrast$_{AP}$, using optimal cutoff point of 1.41, were compared with those of key imaging features known to be specific for AIP (speckled enhancement, halo sign, main pancreatic duct (MPD) tapered narrowing, and duct penetrating sign) and PDA (discrete mass, target appearance, MPD abrupt narrowing, upstream MPD marked dilatation, and pancreatic atrophy).

Results: The lesion contrast differed significantly between AIP and PDA groups at all phases of DCE-MRI (P≤0.008). The maximum difference in the lesion contrast between AIP and PDA (1.23 vs 1.84, P<0.001) and the largest AUROC (0.957) were observed at AP. For AIP, the sensitivity (94.4%) and specificity (87.5%) of Contrast$_{AP}$ (cutoff ≤ 1.41) were comparable or significantly higher than those of all key imaging features (sensitivity, 38.9–88.9% [P≤0.688]; specificity, 48.6–95.8% [P≤0.180]) except for the specificity of halo sign (100%, P=0.004). For PDA, the sensitivity (87.5%) and specificity (94.4%) of Contrast$_{AP}$ (cutoff > 1.41) were also comparable or significantly higher than those of all key imaging features (sensitivity, 40.3–68.1% [P≤0.004]; specificity, 72.2–94.4% [P=0.008–1.000]) except for the sensitivity of discrete mass (95.8%, P=0.031).

Conclusion: Quantitative analysis of the lesion contrast using DCE-MRI, particularly AP, was helpful to differentiate focal-type AIP from PDA. The diagnostic performance of $Contrast_{AP}$ was excellent, and almost comparable or higher than those of the key imaging features.

목차

표 및 그림 차례

Introduction

Autoimmune pancreatitis (AIP) is a rare but distinctive type of chronic pancreatitis, which responds dramatically well to steroid therapy [1]. The radiological and clinical features of AIP can mimic those of pancreatic ductal adenocarcinoma (PDA), and thus differential diagnosis is important to avoid unnecessary surgery in patients with AIP [2-5]. In particular, non-diffuse-type (i.e. focal and multifocal-type) AIP is difficult to be distinguished from PDA at imaging studies unlike diffuse-type AIP that typically manifests as characteristic diffuse sausage-like pancreatic swelling [2-4]. The differential diagnosis of multifocal-type AIP and PDA appears not so difficult since magnetic resonance imaging (MRI) has excellent ability to demonstrate multiple pancreatic masses and multiple pancreatic duct strictures, being highly specific for AIP [6]. For focal-type AIP accounting for 28–48% of all AIP cases [7-10], however, it still remains an extreme challenge to differentiate it from PDA as both diseases manifest as single focal pancreatic mass and single focal pancreatic duct stricture at imaging studies in common.

Recently, many investigators attempted to find differential imaging features between focal-type AIP and PDA using computed tomography (CT) and MRI [11-18]. Previous studies identified some key imaging features, with regard to morphology of the pancreatic mass and pattern of the pancreatic duct stricture, which were important to differentiate the two diseases. Several studies assessed the dynamic enhancement pattern of focal-type AIP using dynamic contrast-enhanced MRI (DCE-MRI); however, the meaningful results mostly focused only on the delayed enhancement [11-14]. The enhancement pattern of focal-type AIP at the arterial phase has never received attention yet. Only a few studies have described merely 'hypointensity' of focal-type AIP at the arterial phase [11-13]. However, we experienced a considerable difference in the enhancement pattern or the lesion contrast at the arterial phase between focal-type AIP and PDA in daily practice. Therefore, we performed this study to quantitatively compare the lesion contrast between focal-type AIP and PDA using DCE-MRI with emphasis on the arterial phase, and to assess the diagnostic performance of the lesion contrast at the arterial phase in differentiating the two diseases.

1

Materials and methods

Study population

This retrospective study was approved by our institutional review board, and patient informed consent was waived. Through a search of our medical database, we identified 169 patients diagnosed with AIP, according to the Asian [19] or HISORt [20] criteria, or international consensus diagnostic criteria [21], in our institution between January 2007 and December 2016 (Fig. 1). Among these, 36 patients (21 men and 15 women; mean age ± standard deviation, 56.7 ± 11.6 years [range, 18–75 years]) were finally included in this study, based on the following inclusion criteria: (a) the presence of DCE-MRI, including unenhanced (UP), arterial (AP), portal (PP), and delayed (DP) phases before steroid treatment; (b) focal-type AIP; (c) the absence of obvious extrapancreatic organ involvement including sclerosing cholangitis, renal involvement, and retroperitoneal fibrosis, which could affect blinded image interpretation; and (d) the presence of normal pancreas parenchyma with normal-appearing signal intensity (SI), which was localized downstream to the mass, and thus available for quantitative analysis. In criterion (b), the focal type was defined as the presence of a single focal mass involving less than half of the total pancreas observed on MRI. The cases with any mass involving more than half of the pancreas (i.e. diffuse type) and the cases with multiple masses involving 2 or more sites (i.e. multifocal type) were excluded from the study.

From January 2013 to December 2015, 782 patients underwent curative-intent surgery for PDA in our institution (Fig. 1). To create a 1:2 matching with the AIP group, we randomly selected 72 (49 men and 23 women; 60.5 ± 9.6 years [40–78 years]) among the 660 patients with PDA who underwent DCE-MRI before surgery, using a commercially available random number generator (QuickCalcs, GraphPad Software). The presence of normal pancreas parenchyma downstream to the mass was also taken into account as stated in criterion (d) of AIP.

MRI techniques

The MRI examinations were performed using a 1.5-T unit (Magnetom Avanto or Vision; Siemens Medical Solutions). The following sequences were used: unenhanced T1-weighted images with fat suppression using a fast low-angle shot; T2-weighted images with fat suppression using respiratory-triggered fast-spin echo or half-Fourier acquisition single-shot turbo spin-echo; MR cholangiopancreatography with thick-slab (40 mm) images using single-shot rapid acquisition with relaxation enhancement sequence during one breath-hold; and DCE T1-weighted images including unenhanced phase (UP) and dynamic triple phases, i.e. arterial (AP), portal (PP), and delayed (DP) phase, using a fat-suppressed spoiled gradient-echo sequence (volumetric interpolated breath-hold examination) at 10 s (arterial phase), 50 s (portal phase), and 3 min (delayed phase) after intravenous injection of gadobenate dimeglumine (MultiHance; Bracco SPA; 0.1 mmol/kg body weight) or gadoteric acid (Dotarem; Guerbet; 0.2 mmol/kg body weight) at a rate of 2 mL/s, using an autoinjector. The detailed scan parameters are summarized in Table 1.

Image analysis

All images were reviewed using a local picture archiving and communication system monitor and digital imaging and communications in medicine imaging software. The patient order was randomized to avoid any patterns in the sequence of the patient categories. The reviewers were blinded to the clinical data, imaging results, and final diagnosis, but were aware that the study population consisted of AIP and PDA.

Analysis of the lesion contrast

For quantitative analysis of the lesion contrast in AIP and PDA, a board-certified abdominal radiologist performed the region-of-interest (ROI) measurement to assess the SI of the pancreatic mass and normal pancreas parenchyma on DCE-MRI. For the pancreatic mass, a round-shaped ROI was carefully placed to encompass as much of the mass as possible on the

image where the mass was most clearly visualized. The peripheral enhancing portion of the mass, if present, was also included in the ROI. For the normal pancreas parenchyma, the largest possible round-shaped ROI was carefully placed in a homogeneous region of the pancreas excluding any recognizable vessels or other non-parenchymal structures, and that was performed in downstream location to the mass to exclude any potential obstructive pancreatitis-related SI change. The SI of the pancreatic mass and the normal pancreas parenchyma were measured 3 times on the same image for each phase, and their average values were calculated to obtain the lesion contrast at each phase using the following equation: Contrast = $SI_{pancreas} / SI_{mass}$.

For qualitative analysis of the lesion contrast, two radiologists, including one who performed the quantitative analysis, reviewed the DCE-MRI to determine in consensus the best phase showing the largest SI difference between the mass and the normal pancreas by visual assessment. They also evaluated whether the lesion contrast changed from UP to AP by visual assessment (decreased, unchanged, or increased).

Analysis of the key imaging features

The same two radiologists reviewed all MRI examinations of the patients to determine in consensus the presence of the following key imaging features for differentiating between focal-type AIP and PDA [11-18,22,23]: discrete pancreatic mass (discernible focal hypointense mass with visible border between the mass and the normal pancreas) on UP and on dynamic triple phases, separately; speckled appearance (speckled hyperintense areas relative to that of the surrounding lesion on UP or AP); target enhancement (layered pattern enhancement, typically hypoenhancing lesion surrounded by hyperenhancement); and delayed enhancement (hypoenhancement on AP and iso- or hyperenhancement on PP or DP compared to the normal pancreas) and its pattern (homogeneous vs. heterogeneous) of the mass; halo sign (thin or thick, continuous, rim-like hypoenhancing soft tissue lesion outlining the pancreas); main pancreatic duct (MPD) stricture and its pattern (abrupt vs. tapered narrowing); duct penetrating sign

4

(visible MPD penetrating the mass without being completely obstructed by the mass); upstream MPD dilatation (absent, mild [< 5 mm], or marked [≥ 5 mm]); and upstream pancreatic atrophy.

Statistical analysis

The lesion contrast obtained by ROI measurement at each phase of DCE-MRI was compared between AIP and PDA groups using Student *t* test. For the lesion contrast at each phase, the receiver operating characteristic (ROC) analysis was performed to compare the area under the ROC curve (AUROC) for differentiating AIP and PDA among the phases. For the phase with the largest AUROC, optimal cutoff point of the lesion contrast to maximize both the sensitivity and specificity on ROC curve (i.e. Youden index) was determined. The sensitivity and specificity of the lesion contrast at the phase when using the optimal cutoff point were compared with those of the key imaging features for the diagnosis of AIP and PDA using McNemar's test. The frequencies of categorical variables regarding the qualitative analysis of the visually assessed lesion contrast and the key imaging features were compared between AIP and PDA groups using chi-squared test or Fisher exact test, as appropriate. P<0.05 was considered statistically significant. SPSS for Windows version 21.0 (IBM Corp., Armonk, NY, USA) and MedCalc for Windows version 12.5.0.0 (MedCalc, Mariakerke, Belgium) was used for the statistical analyses.

Results

Comparison of the lesion contrast between AIP and PDA

The quantitative analysis results regarding the lesion contrast are summarized in Table 2. The lesion contrast differed significantly between AIP and PDA groups at all phases of DCE-MRI (P≤0.008). In AIP, the lesion contrast was highest (mean, 1.49) at UP. Whereas in PDA, the contrast was highest at AP (mean, 1.84). The dynamic pattern of the lesion contrast remarkably

5

differed between the two groups (Fig. 2). In AIP, the lesion contrast, which was highest at UP, gradually decreased as the phase passed. The contrast ultimately declined to less than 1.0 (mean, 0.88) at DP, indicating reversal of SI between the mass and normal parenchyma. In PDA, the lesion contrast increased from UP to AP, and thereafter progressively decreased. The contrast remained 1.0 or higher in majority of the lesions (58 of 72, 80.6%) at DP in contrast with AIP. The maximum difference of the lesion contrast between AIP and PDA was observed at AP (1.23 vs 1.84, P<0.001).

The qualitative analysis results regarding the visually assessed lesion contrast are summarized in Table 3. In AIP, the largest SI difference between the mass and the normal pancreas was observed most frequently at UP (n = 24, 66.7%), followed by DP (n = 7, 19.4%) and AP (n = 5, 13.9%). Whereas in PDA, the largest SI difference between the mass and the normal pancreas was most frequently observed at AP (n = 50, 69.4%). Between UP and AP, the lesion contrast decreased in 26 (72.2%) of 36 patients with AIP, whereas it increased in 56 (77.8%) of 72 patients with PDA. In 10 (27.8%) AIP patients and 8 (11.1%) PDA patients, there were no perceivable contrast changes between UP and AP.

Comparison of the key imaging features for AIP and PDA

The comparison results with regard to the key imaging features for AIP and PDA are summarized in Table 4. The speckled appearance (88.9% vs 51.4%), delayed homogeneous enhancement (80.6% vs 5.6%), halo sign (38.9% vs 0%), MPD tapered narrowing (86.1% vs 27.8%), and duct penetrating sign (38.9% vs 4.2%) were observed significantly more frequently in AIP than in PDA (P<0.001). Meanwhile, discrete mass on AP/PP/DP (95.8% vs 27.8%), target enhancement (68.1% vs 5.6%), MPD abrupt narrowing (63.9% vs 8.3%), upstream MPD marked dilatation (40.3% vs 5.6%), and upstream pancreatic atrophy (51.4% vs 11.1%) were observed significantly more frequently in PDA than in AIP (P<0.001). The discrete mass on UP was more frequently observed in PDA than in AIP (83.3% vs 66.7%),

however, the difference was not statistically significant (P=0.084). Representative cases are presented in Figs. 3 and 4.

Comparison of sensitivity and specificity between the lesion contrast and key imaging features

Among the phases of DCE-MRI, the AUROC of the lesion contrast for differentiating AIP and PDA was largest at AP (0.957) (Table 2). The optimal cutoff point of the lesion contrast at AP ($Contrast_{AP}$) calculated by ROC analysis was 1.41. The sensitivity and specificity of $Contrast_{AP}$ for the diagnosis of AIP using the optimal cutoff point of 1.41 was 94.4% and 87.5%, respectively, and the vice versa for PDA. The comparison of sensitivity and specificity for the diagnosis of AIP and PDA between the $Contrast_{AP}$ when using a cutoff point of 1.41 and the key imaging features is summarized in Table 5. Overall, both the sensitivity and specificity of $Contrast_{AP}$ were mostly comparable or even higher in comparison with those of the key imaging features. More specifically, of the key imaging features for AIP, halo sign was the only one with a specificity significantly higher than that of $Contrast_{AP}$ (100% vs 87.5%, P=0.004). Otherwise, the specificity of $Contrast_{AP}$ for AIP was significantly higher than those of the key imaging features or comparable (87.5% vs 48.6–95.8%, P≤0.180). The sensitivity of $Contrast_{AP}$ for AIP was significantly higher than those of the key imaging features or comparable (94.4% vs 38.9–88.9%, P≤0.688). For PDA, the sensitivity of $Contrast_{AP}$ was significantly higher than those of all key imaging features (87.5% vs 40.3–68.1%, P≤0.004) except for the discrete mass on AP/PP/DP (95.8%, P=0.031), and its specificity was also higher or comparable (94.4% vs 72.2–94.4%, P=0.008–1.000).

Discussion

Our study showed that quantitative analysis of the lesion contrast using DCE-MRI could be helpful in differentiating focal-type AIP from PDA, and especially, the results at AP were the

7

most noticeable. Our findings suggest that $Contrast_{AP}$ can be used as an important quantitative index in differentiating the two diseases in consideration of its excellent diagnostic performance when compared to those of the existing key imaging features. The sensitivity of $Contrast_{AP}$ (94.4%) for AIP (cutoff $\leq$ 1.41) was strikingly higher than that of the halo sign (38.9%). The halo sign is a representative imaging feature of AIP, but the major drawback is poor sensitivity. In recent studies of more than 20 patients with focal-type AIP, the sensitivity of halo sign was very low as 14.6–47.5% [13-15]. The duct penetrating sign also had high specificity (95.8%) but poor sensitivity (38.9%), being very similar to the halo sign. The speckled appearance in AIP is considered to be due to the normal or less affected pancreatic lobules within an inflammatory mass, and has been reported to be specific for AIP in previous studies using CT [15] and MRI [17]. However, in this study, its specificity for AIP was only 48.6%; this is presumably because heterogeneous enhancement of PDA may seem similar to the speckled appearance of AIP. Among the key imaging features of AIP, delayed homogeneous enhancement was the only one with high sensitivity (80.6%) and specificity (94.4%) comparable to $Contrast_{AP}$. A few previous studies comparing the enhancement patterns of focal-type or mass-forming AIP and PDA have also reported high sensitivity and specificity of delayed homogeneous enhancement [11,16,18], and which was highlighted again in our study. Quantitative analysis of the present study also demonstrated a significant difference in delayed enhancement between the two diseases: lesion contrast at DP was less than 1.0 (i.e. $SI_{mass} > SI_{pancreas}$) in 91.7% of AIP, whereas it was 1.0 or higher (i.e. $SI_{mass} \leq SI_{pancreas}$) in 80.6% of PDA. The sensitivity of $Contrast_{AP}$ (87.5%) for PDA (cutoff > 1.41) was significantly higher than those of all key imaging features (40.3–68.1%) except for the discrete mass, while maintaining high specificity (94.4%).

Despite the excellent diagnostic performance of $Contrast_{AP}$, such quantitative analysis might be difficult to apply in actual clinical practice, which is mainly dependent on intuitive decision by the readers based on qualitative analysis. Hence, appropriate qualitative assessment should be supported to enhance the clinical utility of the lesion contrast-related MRI data. Two qualitative factors used to represent $Contrast_{AP}$ of quantitative analysis in this

study were visually-assessed 'best phase showing the largest SI difference between the mass and the normal pancreas' and 'change of the lesion contrast from UP to AP'. The qualitative analysis results were mostly consistent with those of the quantitative analysis. Particularly noteworthy is the change of lesion contrast from UP to AP: the lesion contrast decreased in the majority of AIP, whereas it mostly increased in PDA. The sensitivity and specificity of 'decrease in the visually-assessed lesion contrast from UP to AP' for AIP was 72.2% and 88.9%, respectively. The sensitivity and specificity of 'increase in the visually-assessed lesion contrast from UP to AP' for PDA was 78.8% and 100%, respectively. In other words, between UP and AP, the lesion contrast seldom decreased in PDA, and it increased in none of AIP. Consequently, these findings may be worthy of radiologists' attention as another key imaging feature to differentiate focal-type AIP and PDA, which can be easily applied in today's reading environment where the readers can easily compare the images on UP and AP side by side.

Our results regarding the 'discrete mass' appear to support quantitative and qualitative analysis results of the lesion contrast. The frequency of discrete mass on AP/PP/DP (27.8%) was much lower than that on UP (66.7%) in AIP; this may indicate that it became difficult to distinguish the lesion boundary from the surrounding normal parenchyma throughout the contrast-enhanced images as the lesion enhancement starting from AP was strong to some degree. In contrast, PDA had a higher frequency of discrete mass on AP/PP/DP (95.8%) than on UP (83.3%); and this result may appear that the lesion boundary was more clearly defined on contrast-enhanced images because the lesion enhancement degree was relatively weaker than the normal parenchyma, especially at AP. Several studies have quantitatively analyzed the contrast enhancement using CT in patients with focal-type AIP and PDA, although the lesion contrast was not assessed [9,16,18]. These studies also demonstrated that the degree of contrast enhancement at the arterial or pancreatic phase was greater in AIP than in PDA, which may support our conjecture mentioned above.

The appreciable differences in the lesion contrast at AP between focal-type AIP and PDA may be explained in relation to the following pathological differences of the two diseases as suggested in previous studies [13,17]. In PDA, there is almost no normal pancreatic tissue

remaining inside the mass as the pancreas parenchyma is almost completely replaced by tumor tissue due to carcinogenesis; and tumor-related fibrosis, i.e. desmoplasia is mostly profound. In AIP, the pancreas parenchyma is not totally replaced by the fibrotic mass despite massive lymphoplasmacytic infiltration; acinar cells inside the mass are usually preserved; the lesion distribution is frequently patchy; and interstitial fibrosis is mild [13,17,24,25].

A potential criticism of this study is a discrepancy in the study period between the two patient groups, i.e. 10 years for the AIP group vs. 3 years for the PDA group, which may have caused variations in the quality of MRI examinations for the AIP group. However, a long study period for AIP patients was inevitable owing to the rarity of this disease.

In conclusion, quantitative analysis of the lesion contrast using DCE-MRI, particularly at AP, was helpful to differentiate focal-type AIP from PDA. The diagnostic performance of $Contrast_{AP}$ using optimal cutoff point was excellent and mostly comparable or higher than those of the key imaging features. Therefore, utilization of the $Contrast_{AP}$ in addition to the key imaging features in differentiating the two diseases may improve the diagnostic accuracy and help to establish the prompt and appropriate treatment.

References

1.   Finkelberg DL, Sahani D, Deshpande V, Brugge WR. Autoimmune pancreatitis. N Engl J Med 2006; 355: 2670-6.

2.   Chari ST, Takahashi N, Levy MJ, Smyrk TC, Clain JE, Pearson RK, et al. A diagnostic strategy to distinguish autoimmune pancreatitis from pancreatic cancer. Clin Gastroenterol Hepatol 2009; 7: 1097-103.

3.   Kamisawa T, Imai M, Yui Chen P, Tu Y, Egawa N, Tsuruta K, et al. Strategy for differentiating autoimmune pancreatitis from pancreatic cancer. Pancreas 2008; 37: e62-7.

4.   Kim JH, Kim MH, Byun JH, Lee SS, Lee SJ, Park SH, et al. Diagnostic Strategy for Differentiating Autoimmune Pancreatitis From Pancreatic Cancer: Is an Endoscopic Retrograde Pancreatography Essential? Pancreas 2012;41:639-647.

5.   Kamisawa T, Egawa N, Nakajima H, Tsuruta K, Okamoto A, Kamata N. Clinical difficulties in the differentiation of autoimmune pancreatitis and pancreatic carcinoma. Am J Gastroenterol 2003; 98: 2694-9.

6.   Lee S, Kim JH, Kim SY, Byun JH, Kim HJ, Kim MH, et al. Comparison of diagnostic performance between CT and MRI in differentiating non-diffuse-type autoimmune pancreatitis from pancreatic ductal adenocarcinoma. European Radiology 2018; 2018: 5267-74.

7.   Manfredi R, Frulloni L, Mantovani W, Bonatti M, Graziani R, Mucelli RP. Autoimmune Pancreatitis: Pancreatic and Extrapancreatic MR Imaging-MR Cholangiopancreatography Findings at Diagnosis, after Steroid Therapy, and at Recurrence. Radiology 2011; 260: 428-36.

8.   Rehnitz C, Klauss M, Singer R, Ehehalt R, Werner J, Buchler MW, et al. Morphologic Patterns of Autoimmune Pancreatitis in CT and MRI. Pancreatology 2011; 11: 240-51.

9.   Takahashi N, Fletcher JG, Hough DM, Fidler JL, Kawashima A, Mandrekar JN, et al. Autoimmune pancreatitis: differentiation from pancreatic carcinoma and normal pancreas on the basis of enhancement characteristics at dual-phase CT. AJR Am J Roentgenol 2009; 193: 479-84.

10.   Wakabayashi T, Kawaura Y, Satomura Y, Watanabe H, Motoo Y, Okai T, et al. Clinical and imaging features of autoimmune pancreatitis with focal pancreatic swelling or mass formation: comparison with so-called tumor-forming pancreatitis and pancreatic carcinoma. Am J Gastroenterol 2003; 98: 2679-87.

11.   Choi SY, Kim SH, Kang TW, Song KD, Park HJ, Choi YH. Differentiating Mass-Forming Autoimmune Pancreatitis From Pancreatic Ductal Adenocarcinoma on the Basis of Contrast-Enhanced MRI and DWI Findings. American Journal of Roentgenology 2016; 206: 291-300.

12.   Hur BY, Lee JM, Lee JE, Park JY, Kim SJ, Joo I, et al. Magnetic resonance imaging findings of the mass-forming type of autoimmune pancreatitis: Comparison with pancreatic adenocarcinoma. J Magn Reson Imaging 2012; 36: 188-97.

13.   Kim M, Jang KM, Kim JH, Jeong WK, Kim SH, Kang TW, et al. Differentiation of mass-forming focal pancreatitis from pancreatic ductal adenocarcinoma: value of characterizing dynamic enhancement patterns on contrast-enhanced MR images by adding signal intensity color mapping. European Radiology 2017; 27: 1722-32.

14.   Negrelli R, Manfredi R, Pedrinolla B, Boninsegna E, Ventriglia A, Mehrabi S, et al. Pancreatic duct abnormalities in focal autoimmune pancreatitis: MR/MRCP imaging findings. European Radiology 2015; 25: 359-67.

15.   Furuhashi N, Suzuki K, Sakurai Y, Ikeda M, Kawai Y, Naganawa S. Differentiation of focal-type autoimmune pancreatitis from pancreatic carcinoma: assessment by multiphase contrast-enhanced CT. European Radiology 2015; 25: 1366-74.

16.	Muhi A, Ichikawa T, Motosugi U, Sou H, Sano K, Tsukamoto T, et al. Mass-forming autoimmune pancreatitis and pancreatic carcinoma: Differential diagnosis on the basis of computed tomography and magnetic resonance cholangiopancreatography, and diffusion-weighted imaging findings. Journal of Magnetic Resonance Imaging 2012; 35: 827-36.

17.	Sugiyama Y, Fujinaga Y, Kadoya M, Ueda K, Kurozumi M, Hamano H, et al. Charac-teristic magnetic resonance features of focal autoimmune pancreatitis useful for differentiation from pancreatic cancer. Japanese Journal of Radiology 2012; 30: 296-309.

18.	Sun GF, Zuo CJ, Shao CW, Wang JH, Zhang J. Focal autoimmune pancreatitis: radiological characteristics help to distinguish from pancreatic cancer. World J Gastroenterol 2013; 19: 3634-41.

19.	Otsuki M, Chung JB, Okazaki K, Kim MH, Kamisawa T, Kawa S, et al. Asian diagnostic criteria for autoimmune pancreatitis: consensus of the Japan-Korea Symposium on Autoimmune Pancreatitis. J Gastroenterol 2008; 43: 403-8.

20.	Chari ST, Smyrk TC, Levy MJ, Topazian MD, Takahashi N, Zhang L, et al. Diagnosis of autoimmune pancreatitis: the Mayo Clinic experience. Clin Gastroenterol Hepatol 2006; 4: 1010-6; quiz 1934.

21.	Shimosegawa T, Chari ST, Frulloni L, Kamisawa T, Kawa S, Mino-Kenudson M, et al. International consensus diagnostic criteria for autoimmune pancreatitis: guidelines of the International Association of Pancreatology. Pancreas 2011; 40: 352-8.

22.	Carbognin G, Girardi V, Biasiutti C, Camera L, Manfredi R, Frulloni L, et al. Autoimmune pancreatitis: imaging findings on contrast-enhanced MR, MRCP and dynamic secretin-enhanced MRCP. Radiologia Medica 2009; 114: 1214-31.

23.	Chang WI, Kim BJ, Lee JK, Kang P, Lee KH, Lee KT, et al. The Clinical and Radiological Characteristics of Focal Mass-Forming Autoimmune Pancreatitis Comparison With Chronic Pancreatitis and Pancreatic Cancer. Pancreas 2009; 38: 401-8.

24.   Kim HJ, Kim YK, Jeong WK, Lee WJ, Choi D. Pancreatic duct "Icicle sign" on MRI for distinguishing autoimmune pancreatitis from pancreatic ductal adenocarcinoma in the proximal pancreas. European Radiology 2015; 25: 1551-60.

25.   Chandan VS, Iacobuzio-Donahue C, Abraham SC. Patchy distribution of pathologic abnormalities in autoimmune pancreatitis: implications for preoperative diagnosis. The American journal of surgical pathology 2008; 32: 1762-9.

Table 1. MRI sequences and parameters

	Transverse T2-weighted		MRCP	Transverse T1-weighted	
	HASTE	RT-TSE	Single-shot RARE	FLASH	VIBE
IV contrast enhancement	Pre-contrast	Pre-contrast	Pre-contrast	Pre-contrast	Pre- & Post-contrast
TR/TE (msec)	Infinite/154	3600-5100/96	Infinite/1000	224/2.5	4.1-4.2/1.5-1.7
Flip angle (˚)	150	150	180	70	10
Field of view (mm)	240 × 350	240 × 350	300 × 300	240 × 350	280 × 350
Matrix	192 × 256	264 × 384	320 × 320	176 × 256	256 × 320
Slice thickness (mm)	6	6	40	6	4
Interslice gap (mm)	1.2	1.2	0	1.2	0
Echo train length	256	13	256	NA	NA

Note. For all pulse sequences, fat saturation was employed using the chemical shift-selective fat suppression technique.

Abbreviations: MRCP, magnetic resonance cholangiopancreatography; HASTE, half-Fourier acquisition single-shot turbo spin-echo; RT-TSE, respiratory-triggered turbo spin-echo; RARE, rapid acquisition with relaxation enhancement; FLASH, fast low-angle shot; VIBE, volumetric interpolated breath-hold examination; TR, repetition time; TE, echo time; NA, not applicable.

Table 2. Quantitative analysis of the lesion contrast by ROI measurement

	AIP (n=36)	PDA (n=72)	P value	AUROC[#]	P value*
Contrast$_{UP}$, mean [range, SD]	1.49 [1.15–2.03, 0.21]	1.60 [1.23–2.06, 0.19]	0.008	0.651 [0.553–0.740]	<0.001
Contrast$_{AP}$, mean [range, SD]	1.23 [0.95–1.73, 0.16]	1.84 [1.25–3.16, 0.38]	<0.001	0.957 [0.900–0.987]	
Contrast$_{PP}$, mean [range, SD]	1.00 [0.79–1.28, 0.13]	1.44 [0.98–2.11, 0.28]	<0.001	0.940 [0.877–0.976]	0.407
Contrast$_{DP}$, mean [range, SD]	0.88 [0.71–1.15, 0.10]	1.21 [0.76–1.84, 0.25]	<0.001	0.910 [0.839–0.956]	0.111

[#] Area under receiver operating characteristic curve for differentiating AIP and PDA [95% confidence interval]
* Compared with AUROC of Contrast$_{AP}$

Table 3. Qualitative analysis of the lesion contrast by visual assessment

	AIP (n=36) (%)	PDA (n=72) (%)	P value
Best phase[#]			<0.001
Unenhanced phase	24 (66.7)	15 (20.8)	
Arterial phase	5 (13.9)	50 (69.4)	
Portal phase	0 (0)	3 (4.2)	
Delayed phase	7 (19.4)	4 (5.6)	
Contrast change*			<0.001
Decreased	26 (72.2)	8 (11.1)	
Unchanged	10 (27.8)	8 (11.1)	
Increased	0 (0)	56 (77.8)	

[#] Best phase showing the largest SI difference between the mass and the normal pancreas

* Change of the lesion contrast from unenhanced phase to arterial phase

Table 4. Comparison of the key imaging features for AIP and PDA

	AIP (n=36) (%)	PDA (n=72) (%)	P value
Discrete mass on UP	24 (66.7)	60 (83.3)	0.084
Discrete mass on AP/PP/DP	10 (27.8)	69 (95.8)	<0.001
Speckled appearance	32 (88.9)	37 (51.4)	<0.001
Target enhancement	2 (5.6)	49 (68.1)	<0.001
Delayed enhancement			<0.001
Absent	2 (5.6)	24 (33.3)	
Homogeneous	29 (80.6)	4 (5.6)	
Heterogeneous	5 (13.9)	44 (61.1)	
Halo sign	14 (38.9)	0 (0)	<0.001
MPD stricture			<0.001
Absent	2 (5.6)	6 (8.3)	
Tapered	31 (86.1)	20 (27.8)	
Abrupt	3 (8.3)	46 (63.9)	
Duct penetrating sign	14 (38.9)	3 (4.2)	<0.001
Upstream MPD dilatation			<0.001
Absent	18 (50)	13 (18.1)	
Mild (< 5 mm)	16 (44.4)	30 (41.7)	
Marked (≥ 5 mm)	2 (5.6)	29 (40.3)	
Upstream pancreatic atrophy	4 (11.1)	37 (51.4)	<0.001

Abbreviations: UP, unenhanced phase; AP, arterial phase; PP, portal phase; DP, delayed phase;

MPD, main pancreatic duct

Table 5. Comparison of sensitivity and specificity for the diagnosis of AIP and PDA between Contrast$_{AP}$ and key imaging features

AIP	Sensitivity	P value*	Specificity	P value*
Contrast$_{AP}$ ≤ 1.41[#]	94.4%		87.5%	
Speckled appearance	88.9%	0.688	48.6%	<0.001
Delayed homogeneous enhancement	80.6%	0.180	94.4%	0.180
Halo sign	38.9%	<0.001	100%	0.004
MPD tapered narrowing	86.1%	0.453	72.2%	0.035
Duct penetrating sign	38.9%	<0.001	95.8%	0.146

| PDA	Sensitivity	P value*	Specificity	P value*
Contrast$_{AP}$ > 1.41[#]	87.5%		94.4%	
Discrete mass on AP/PP/DP	95.8%	0.031	72.2%	0.008
Target enhancement	68.1%	0.004	94.4%	1.000
MPD abrupt narrowing	63.9%	0.003	91.7%	1.000
MPD marked dilatation	40.3%	<0.001	94.4%	1.000
Upstream pancreatic atrophy	51.4%	<0.001	88.9%	0.688

[#] Optimal cutoff point calculated by ROC analysis

* Compared with Contrast$_{AP}$

Abbreviations: MPD, main pancreatic duct; AP, arterial phase; PP, portal phase; DP, delayed phase
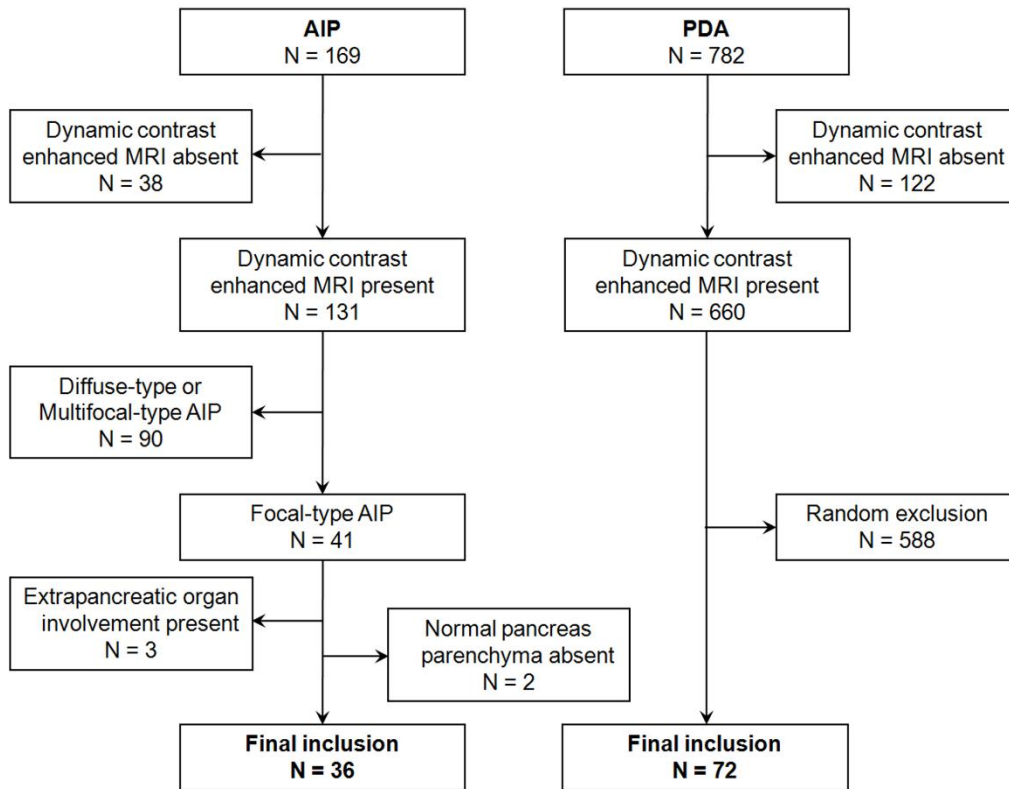
**Fig. 1.** Flow diagram showing the selection of the study population.
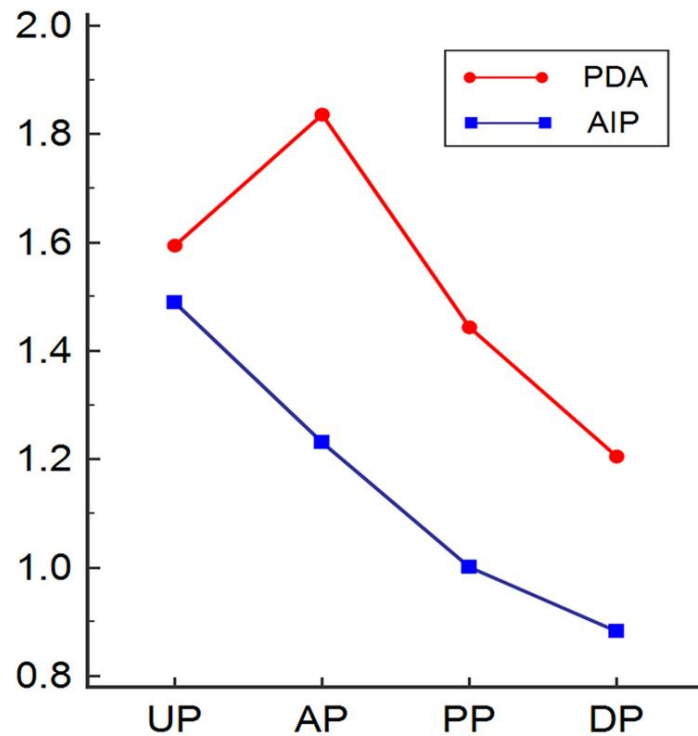
Fig. 2. Dynamic pattern of the lesion contrast in focal-type AIP and PDA.

Horizontal and vertical axis indicates the phases of DCE-MRI (UP, unenhanced phase; AP, arterial phase; PP, portal phase; and DP, delayed phase) and the mean value of the lesion contrast (SIpancreas/SImass), respectively. In AIP, the lesion contrast is highest at UP and it gradually decreases as the phase passes, being less than 1.0 (mean, 0.88) at DP. In PDA, the lesion contrast increases between UP and AP, and thereafter progressively decreased. Note that the maximum difference of the lesion contrast between AIP and PDA is observed at AP (1.23 vs. 1.84, P<0.001).
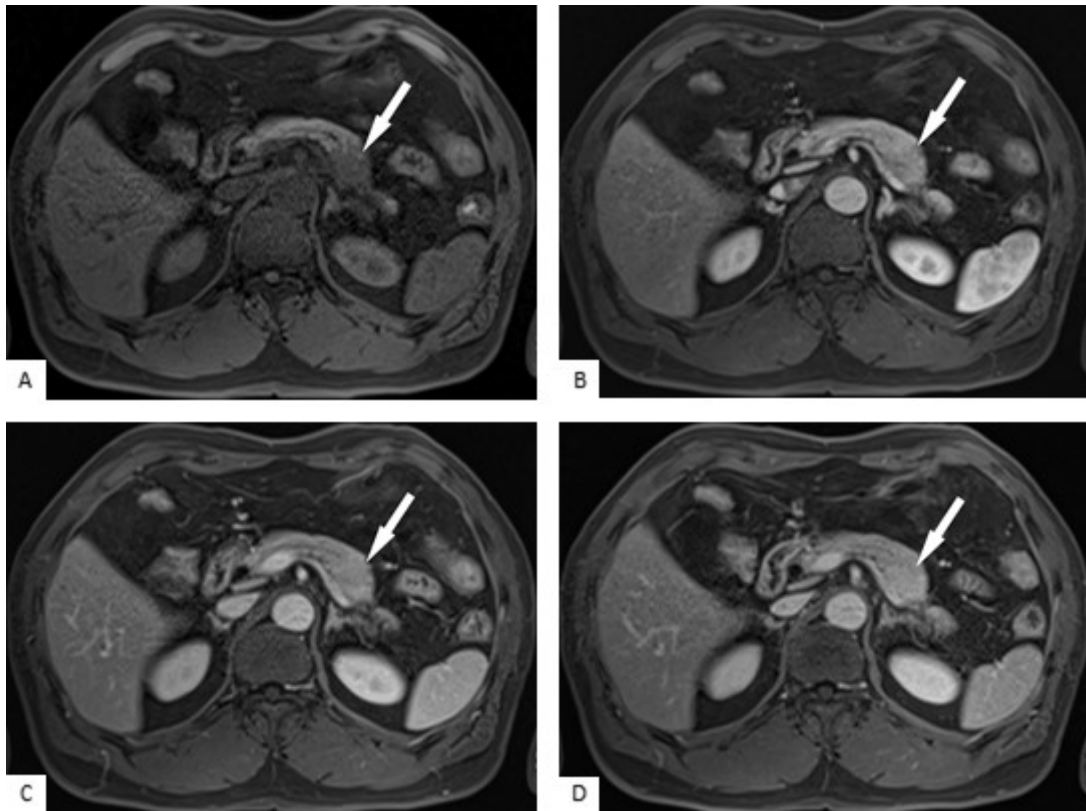
Fig. 3. A 59-year-old man with focal-type AIP.

The pancreatic mass (arrows) in the tail appears discrete hypointensity on unenhanced phase (A) and ill-defined, subtle hypo- or isointensity on arterial phase (B). The lesion contrast (SIpancreas/SImass) remarkably decreased between unenhanced (1.75) and arterial (1.03) phase. The portal (C) and delayed (D) phase images clearly demonstrate homogeneous hyperintensity of the mass.
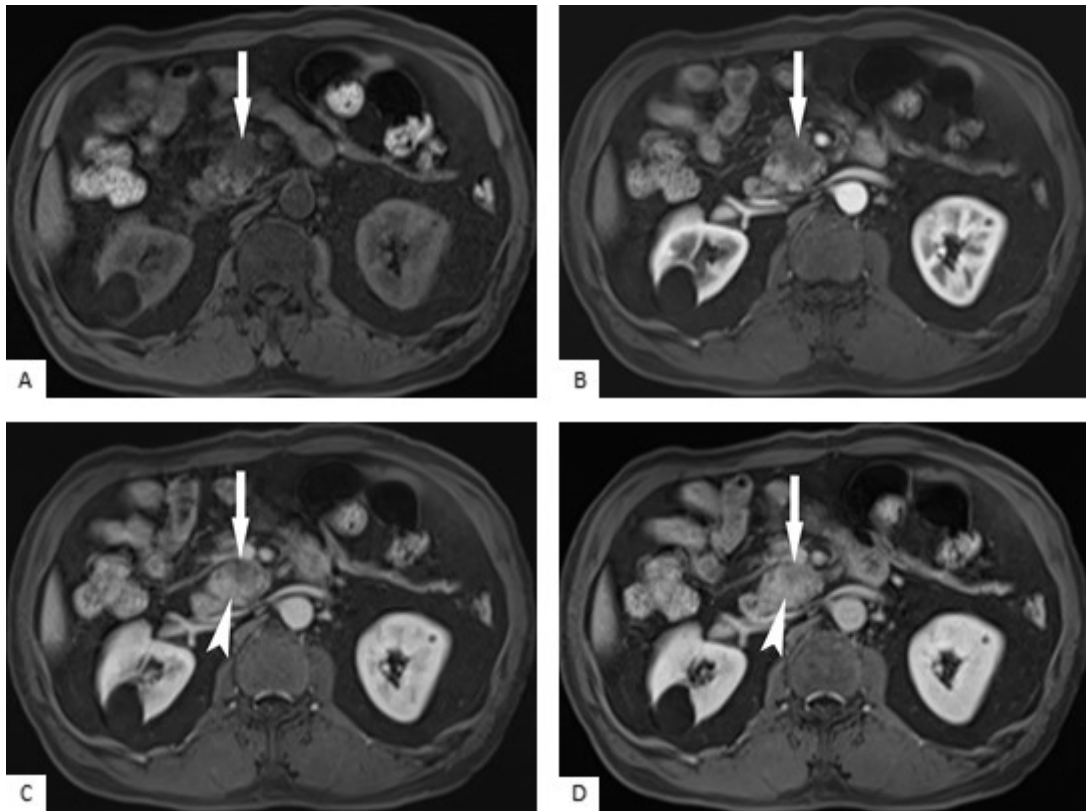
Fig. 4. A 69-year-old man with PDA.

The pancreatic mass (arrows) in the head appears discrete hypointensity on both unenhanced (A) and arterial (B) phase. However, the lesion contrast (SIpancreas/SImass) increased between unenhanced (1.73) and arterial (2.33) phase, and thus the mass appears more conspicuous on arterial phase than on unenhanced phase. During the portal (C) and delayed (D) phase, the mass progressively enhances and the lesion periphery (arrowheads) appears iso- or mild hyperintensity, but the lesion center still maintains hypointensity.

국문요약

국소형 자가면역 췌장염과 췌장선암의 감별진단: 역동적 조영증강 자기공명 영상에서 동맥기를 중심으로 병변 대조도의 정량적 비교 연구

권지혜, 김진희

울산대학교 의과대학 서울아산병원 영상의학과

연구목적: 역동적 조영증강 자기공명 영상 (dynamic contrast-enhanced MR imaging, DCE-MRI)을 이용하여 동맥기 영상에 초점을 두고 국소형 자가면역 췌장염 (autoimmune pancreatitis, AIP)와 췌장암 (pancreatic ductal adenocarcinoma, PDA)의 병변 대조도를 정량적으로 비교하고자 하였다. 또한 두 질환의 감별하는데 있어서 동맥기 병변 대조도 ($Contrast_{AP}$)의 진단적 유용성을 평가하고자 하였다.

연구방법: 36 명의 국소형 AIP 환자와 72 명의 수술적으로 절제된 PDA 환자를 포함하였다. 이들은 조영증강 전, 동맥기, 문맥기, 지연기 영상을 모두 포함하는 DCE-MRI 를 시행하였다. 각 시기 (phase)의 영상에서 종괴와 정상 췌장의 신호 강도 (signal intensity, SI)를 측정하였다. 이를 이용하여 각 시기에서 AIP 와 PDA 두 군의 병변 대조도 ($SI_{pancreas}/SI_{mass}$)를 비교하였다. 각 시기에서 병변 대조도의 진단적 유용성을 비교하기 위하여 수신자 조작 특성 곡선 아래 면적 (area under the receiver operating characteristic curve, AUROC)을 이용하였다. 최적 기준치인 1.41 을 적용하여 $Contrast_{AP}$ 의 민감도와 특이도를 구하였다. 이를 AIP 에 특이적인 주요 영상 소견인 점상 조영증강 (speckled enhancement), 달무리 징후 (halo sign), 점차 가늘어지는 (tapered) 주췌관 협착, 췌관 통과 징후 (duct penetrating sign)의 민감도 및 특이도와 비교하였다. 또한 이를 PDA 에 특이적인 주요 영상 소견인 뚜렷한 종괴 (discrete mass), 과녁 징후 (target sign), 갑작스러운 (abrupt) 주췌관 협착, 상류 주췌관의 현저한 확장, 상류 췌장 실질 위축 소견의 민감도 및 특이도와도 비교하였다.

연구결과: DCE-MRI 의 모든 시기에서 AIP 군과 PDA 군의 병변 대조도는 유의한 차이를 보였다 (P≤0.008). 동맥기 영상에서 AIP 와 PDA 의 병변 대조도에 가장 큰 차이를 보였으며 (1.23 vs 1.84, P<0.001), $Contrast_{AP}$ 가 가장 큰 AUROC 값을 보였다 (0.957). $Contrast_{AP}$ (cutoff ≤ 1.41)의 AIP 에 대한 민감도 (94.4%) 및 특이도 (87.5%)는 달무리 징후 (halo sign)의 특이도 (100%, P=0.004)를 제외한 모든 AIP 주요 영상 소견들의 민감도 및 특이도 (민감도, 38.9–88.9% [P≤0.688]; 특이도, 48.6–95.8% [P≤0.180])에 비해 더 높거나 유사하였다. $Contrast_{AP}$ (cutoff> 1.41)의 PDA 에 대한 민감도 (87.5%) 및 특이도 (94.4%)는 뚜렷한 종괴 (discrete mass)의 민감도 (95.8%, P=0.031)를 제외한 모든 PDA 주요 영상 소견들의 민감도 및 특이도 (민감도, 40.3–68.1% [P≤0.004]; 특이도, 72.2–94.4% [P=0.008–1.000])에 비해 더 높거나 유사하였다.

연구결론: DCE-MRI 를 이용하여 특히 동맥기 영상에서 병변 대조도를 정량적으로 분석하는 것은 국소형 AIP 와 PDA 를 감별하는 데 도움이 된다. $Contrast_{AP}$ 는 두 질환의 감별에 매우 유용하며, 대부분의 AIP 와 PDA 의 주요 영상 소견들과 비교하였을 때 진단적 유용성이 유사하거나 더 우수하다.

중심단어 췌장염 · 자가면역성 질환 · 췌장선암 · 자기공명영상